24th INTERNATIONAL CONGRESS ON SOUND AND VIBRATION
23–27 July 2017, London

ACTIVE CONTROL OF LATERAL VIBRATION OF A SHAFT-HULL COUPLED SYSTEM

Hui Qin, Hongbo Zheng, Wenyuan Qin

Shanghai Jiao Tong University, Institute of Vibration Shock & Noise, Shanghai, China
email: narlia525@sjtu.edu.cn

Zhiyi Zhang

Shanghai Jiao Tong University, Institute of Vibration Shock & Noise, Shanghai, China

Collaborative Innovation Center for Advanced Ship and Deep-Sea Exploration, Shanghai, China

A propulsion shafting system can excite the hull structure through its bearings and resultingly induces vibrations in the hull. To suppress lateral vibration transmission, a new method using electromagnetic bearings in the shafting system is proposed. For the purpose of theoretical investigation, dynamic characteristics of the electromagnetic bearing are analyzed at first, and subsequently a dynamic model of the shafting-hull coupled system is established to derive the frequency response functions with the help of the Frequency Response Synthesis method, and finally the influence of the electromagnetic bearing stiffness and damping on the vibration of the shafting-hull system is evaluated. Simulation results demonstrate that the proposed approach is effective in suppressing vibration transmission in the shafting system and can be regarded as an optional method for systematic vibration control of shafting-hull systems.
Keywords: propulsion shafting, lateral vibration, electromagnetic bearing, vibration control

1. Introduction

A propulsion shafting system excites the hull structure through its bearings and causes acoustic radiation [1]. By controlling vibration transmission through the bearings, it is possible to decrease vibration and acoustic radiation. So far a lot of researches on the longitudinal vibration control of propulsion shafting systems have been conducted [2-5], but the control of lateral vibration transmission is much less reported. Most of the investigations on the lateral vibration of shafting are focused on natural frequencies, calculation of whirling vibration and so on [6-9].

Electromagnetic bearings (EMBs) are widely used for various purposes primarily due to the advantages of being free of friction and low maintenance costs. Dynamics of electromagnetic bearings depend mainly on the implemented control laws, and for active magnetic bearings, the stiffness and damping are adjustable. Therefore, it is possible to change the stiffness and damping to meet actual operation requirements and even the rotor speed within physical limits [10-11]. A variety of controllers for electromagnetic bearings have been proposed [12-17], and good performance has been achieved. Electromagnetic bearings are mainly used in flywheel energy storage system [18], high-speed grinding spindle [19], turbomachinery [20], and so on. However, no investigation has been reported in lateral vibration control of propulsion shafting systems.

In this paper, a new concept of using EMBs in shafting systems to control lateral vibration transmission is proposed. For theoretical investigation, a propulsion shafting containing a rear bearing, a front bearing and a thrust bearing is adopted. In this system, the rear and front bearings are water-lubricated rubber bearings that may cause intensive vibration in the low-speed condition due to poor lubrication. In this paper, an EMB is adopted to work in parallel with the rear bearing in order to

reduce friction and the lateral vibration transmission. The lateral vibration frequencies change within a certain range for adaptable stiffness and damping of the bearing. As a result, proper impedances can be achieved at different rotor speeds, and vibration transmission from the shaft to the hull can be reduced.

2. Stiffness and damping of an electromagnetic bearing

The main components as well as the operation principle of a simple EMB are depicted in Fig.1, where the sensors measure displacements of the rotor from its reference position and the controller sends control signals that are amplified by power amplifiers in order to generate necessary currents for the bearing. As a result, magnetic fields in the electromagnetic bearing and desired magnetic forces acting on the rotor are generated. A closed loop control is realized and the system is stabilized under a feedback control law. The stiffness, damping and stability of the system depend mainly on the implemented control law.

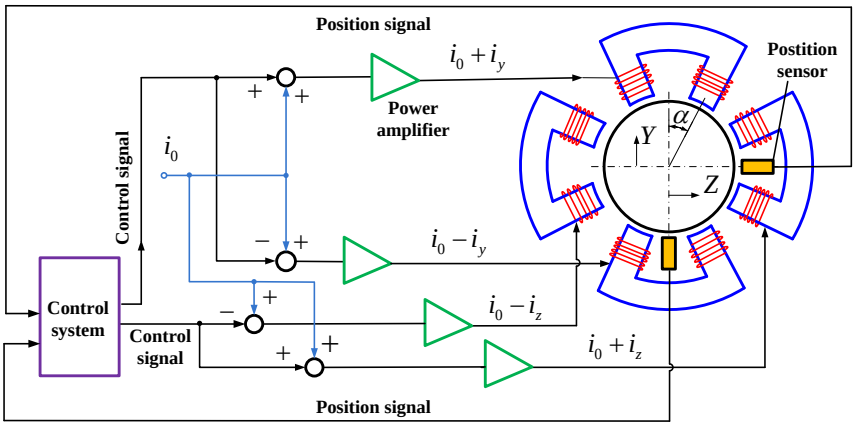

Figure 1 : Differential driving mode of 2-DOF electromagnetic bearing.

The differential driving mode of a 2-DOF electromagnetic bearing is illustrated in Fig.1. In order to simplify control of the electromagnetic bearing, four pairs of coils or eight magnetic poles are commonly used in a radial magnetic bearing and they are assumed to have identical structures. The magnetic poles are placed symmetrically with symmetric power amplifier circuits, which enables the bearing to attract the rotor along two orthogonal and decoupled axes. i_0 is the bias current while i_y and i_z are the control currents in the vertical (Y) and the horizontal (Z) directions, respectively. In the case of differential driving mode, one pair of magnetic poles are driven by the sum of the bias current and the control current, and the other by the difference.

If the eddy current loss, flux leakage and saturation of the core material are neglected, the total magnetic force along the Y direction can be described as

$$F_y = k\left[\frac{(i_0 + i_y)^2}{(s_0 - y)^2} - \frac{(i_0 - i_y)^2}{(s_0 + y)^2}\right]\cos\alpha \tag{1}$$

where $k = \mu_0 N^2 A_a / 4$, α is half of the angle between two adjacent magnetic poles, μ_0 represents the permeability of air, s_0 is the nominal air gap, y is the deviation of air gap, A_a is the cross-section of the air gap, and N is the number of coil windings.

The magnetic force can be linearized with respect to the control current and deviation of the air gap by using Taylor's series in the case of $y << s_0$ and $i_y << i_0$ as

$$F_y \approx k_i i_y + k_s y \tag{2}$$

where $k_i = \frac{4ki_0}{s_0^2}\cos\alpha$ is the force-current factor and $k_s = \frac{4ki_0^2}{s_0^3}\cos\alpha$ is the force-displacement factor.

If the magnetic forces are equivalent to spring and damping forces, and a PID controller is used, the equivalent stiffness and damping can be given as

$$K = k_i c_p + k_s, C = k_i (c_d - \frac{c_i}{\omega^2}) \tag{3}$$

where c_p, c_i, c_d are the corresponding parameters of the PID controller.

Equation (3) indicates that the stiffness is related to the proportional factor while the damping is related to the integral factor, the derivative factor as well as the frequency. Hence, when an electromagnetic bearing is applied to a shafting system, theoretical analysis can be simplified by considering the equivalent stiffness and damping only.

3. Mathematical model

For complicated systems like the shaft-hull system shown in Fig.3, it is difficult to obtain a dynamic model by analytic methods, and it is also inconvenient to explore the influence of parameters by numerical methods. The shaft-hull system includes two elastic bodies, i.e. the shaft and the hull, and they are connected with springs. Parameters of the springs are listed in Table 1. In this section, the finite element method is used to derive the FRFs of the shaft and the hull, respectively, and the FRF synthesis method is applied to establish the dynamic model of the coupled system.

The finite element model of the shaft-hull system is shown in Fig. 2. In this model, the shaft is modelled by beam elements and the propeller by a rigid body element of mass and moment inertia. The hull is composed of a cylindrical shell, a conic shell and an ellipsoidal shell. They are all reinforced with stiffeners. The stiffeners include longitudinal bars between the cylindrical shell and the conic shell, and ring stiffeners arranged evenly along the longitudinal direction.

(a) **(b)**

Figure 2: (a) Finite element model of the shaft-hull system. (b) Finite element model of the hull system.

Table 1: Springs of the shaft-hull system

Bearing	Point	Position	Displacement	Stiffness	Force
Rear bearing	1	Shaft	$\bar{y}_1, \bar{z}_1$	$k_{1y} = 3.6e8\,\mathrm{N/m}$, $k_{1z} = 9e7\,\mathrm{N/m}$	Q_{1y}, Q_{1z}
	4	Hull	y_1, z_1		
Front bearing	2	Shaft	$\bar{y}_2, \bar{z}_2$	$k_{2y} = 3e8\,\mathrm{N/m}$, $k_{2z} = 3e7\,\mathrm{N/m}$	Q_{2y}, Q_{2z}
	5	Hull	y_2, z_2		
Thrust bearing	3	Shaft	$\bar{x}_3, \bar{y}_3, \bar{z}_3$	$k_{3x} = 1e9\,\mathrm{N/m}$, $k_{3y} = 3e9\,\mathrm{N/m}, k_{3z} = 3e9\,\mathrm{N/m}$	Q_{3x}, Q_{3y}, Q_{3z}
	6	Hull	x_3, y_3, z_3		

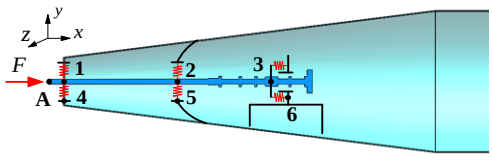

Figure 3: Simplified model of the shaft-hull system.

The vertical and horizontal displacements of Point 2 at the shaft and Point 5 at the hull can be expressed as

$$\begin{cases} \bar{y}_2 = -H_{yy}(2,1)Q_{1y} - H_{yy}(2,2)Q_{2y} - H_{yy}(2,3)Q_{3y} + H_{yy}(2,A)F_y \\ \bar{z}_2 = -H_{zz}(2,1)Q_{1z} - H_{zz}(2,2)Q_{2z} - H_{zz}(2,3)Q_{3z} + H_{zz}(2,A)F_z \\ y_2 = H_{yy}(5,4)Q_{1y} + H_{yz}(5,4)Q_{1z} + H_{yy}(5,5)Q_{2y} + H_{yz}(5,5)Q_{2z} + H_{yx}(5,6)Q_{3x} + H_{yy}(5,6)Q_{3y} + H_{yz}(5,6)Q_{3z} \\ z_2 = H_{zy}(5,4)Q_{1y} + H_{zz}(5,4)Q_{1z} + H_{zy}(5,5)Q_{2y} + H_{zz}(5,5)Q_{2z} + H_{zx}(5,6)Q_{3x} + H_{zy}(5,6)Q_{3y} + H_{zz}(5,6)Q_{3z} \end{cases} \tag{4}$$

where $H_{yy}(m,n)$, $H_{yz}(m,n)$, $H_{yx}(m,n)$, $H_{zy}(m,n)$, $H_{zz}(m,n)$ and $H_{zx}(m,n)$ represent the FRFs between Point *m* and Point *n*, and the subscript *x*, *y* and *z* denote the directions of the displacements and forces. Similarly, displacements of points 1, 4, 3 and 6 can also be represented by forces and FRFs.
According to the continuity of displacements and the equilibrium condition of forces, the following equations exist

$$\begin{cases} k_{1y}(\bar{y}_1 - y_1) = Q_{1y}, k_{1z}(\bar{z}_1 - z_1) = Q_{1z} \\ k_{2y}(\bar{y}_2 - y_2) = Q_{2y}, k_{2z}(\bar{z}_2 - z_2) = Q_{2z} \\ k_{3x}(\bar{x}_3 - x_3) = Q_{3x}, k_{3y}(\bar{y}_3 - y_3) = Q_{3y}, k_{3z}(\bar{z}_3 - z_3) = Q_{3z} \end{cases} . \tag{5}$$

Equations (4) and (5) can be replaced by a matrix equation

$$H_Q \cdot Q = H_F \cdot F \tag{6}$$

where $Q = \{Q_{1y}, Q_{1z}, Q_{2y}, Q_{2z}, Q_{3x}, Q_{3y}, Q_{3z}\}^T$ is the interfacial force vector, $F = \{F_x, F_y, F_z\}^T$ is the disturbance force vector, H_Q is a 7-by-7 matrix, H_F is a 7-by-3 matrix, and the elements of both matrices are the FRFs of points 1-6 and A, as shown in Fig. 3.

In addition, if the viscous damping *c* is introduced, the stiffness *k* in Eq. (5) will be replaced by $k+j\omega c$, where $j^2=-1$ and ω is the angular frequency. And if the structure damping η is introduced, the stiffness *k* in Eq. (5) will be replaced by $k+j\eta$, which means that the stiffness is complex stiffness. If the disturbance forces are given, the interfacial forces can be calculated from Eq. (6) and the displacements can be calculated from Eq. (4) , respectively. Therefore, FRFs of the coupled system can be obtained from these equations.

4. Simulation results

In the shaft-hull system, the EMB is placed in parallel with the rear bearing. Theoretically, when the EMB is used in the shaft-hull system, various equivalent stiffness can be acquired by adjusting the control parameters, which changes vibration transmission. As shown in Fig. 4, when the EMB is controlled with damping, the peak amplitudes of the acceleration responses will be decreased, which will achieve better performance in the vibration control. So, in the following, when the EMB is introduced into the shaft-hull system, it will be controlled with damping.

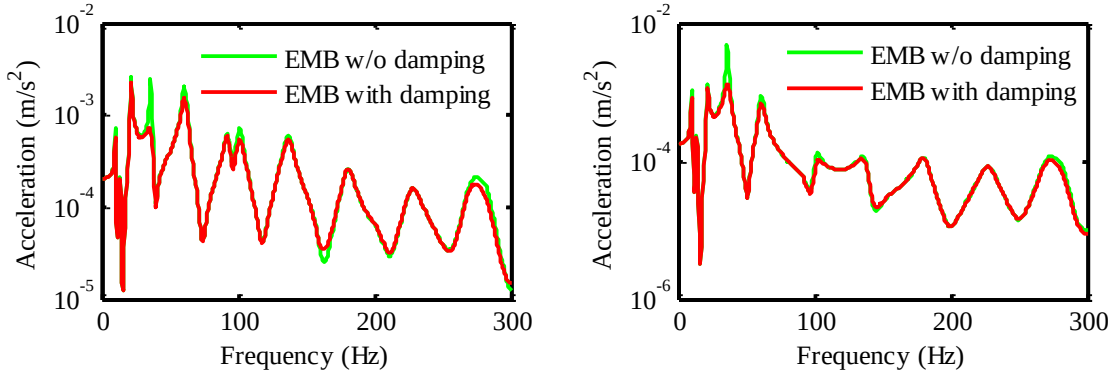

(a) Rear bearing. **(b) Front bearing.**

Figure 4: Vertical acceleration responses of the rear and front bearing to the unit vertical force.

When the EMB is located in parallel with the rear support, the parameters of the bearing are given as

$$i_0=15\text{ A},\ s_0=1.5\text{ mm},\ \alpha=\pi/8,\ \mu_0=4\pi\times10^{-7}\text{ H/m},\ N=300,\ A_a=324\text{ cm}^2,$$
$$c_{py}=11595.1\text{ A/m},\ c_{pz}=10398.8\text{ A/m},\ c_{dy}=319.0\text{ A}\cdot\text{s/m},\ c_{dz}=79.8\text{ A}\cdot\text{s/m}.$$

The vertical unit excitation force is applied at point A, and the force responses in the vertical and horizontal directions of the rear, front and thrust bearings are calculated and shown in Figs. 5, 6 and 7 respectively. As illustrated by these curves, the interfacial forces at the three bearings decline remarkably in the whole. But the vertical forces at the front and the thrust bearings will be magnified at about 275 Hz which is the bending mode of the hull. In addition, in the frequency range of 0.5-21.5 Hz which is the bending mode of the hull, the forces responses keep roughly unchanged and the peak amplitudes are reduced to some extent.

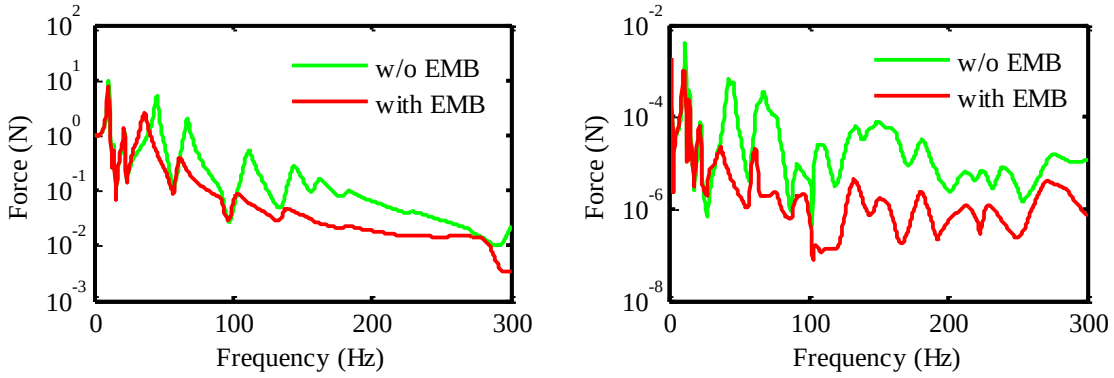

(a) Vertical. **(b) Horizontal.**

Figure 5: Vertical and horizontal force responses of rear bearing to the unit vertical force.

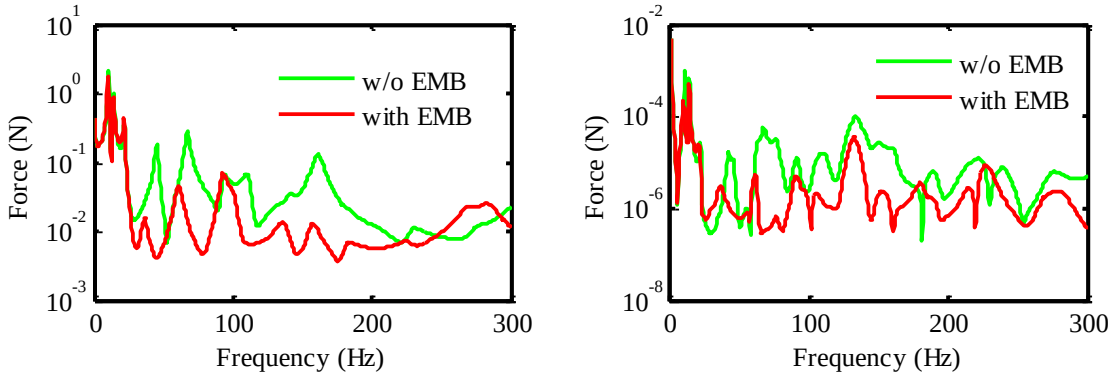

(a) Vertical. **(b) Horizontal.**

Figure 6: Vertical and horizontal force responses of front bearing to the unit vertical force.

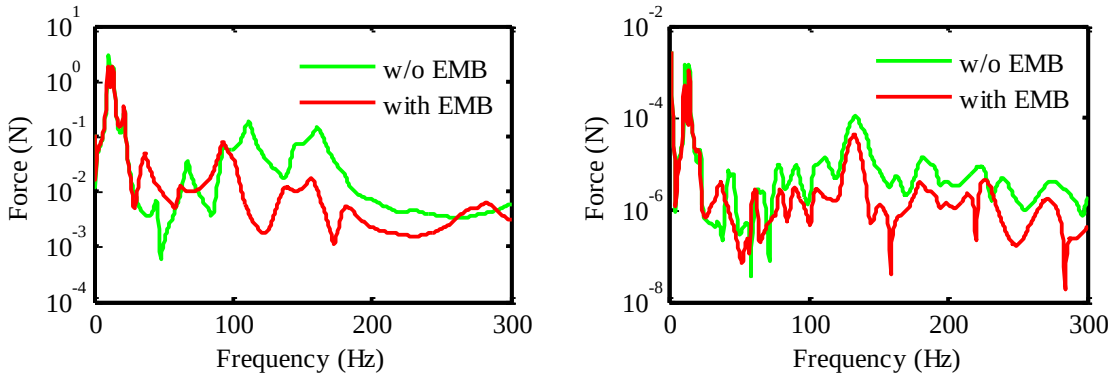

(a) Vertical. **(b) Horizontal.**

Figure 7: Vertical and horizontal force responses of thrust bearing to the unit vertical force.

Comparison of the acceleration responses at the rear, front and thrust bearings with or without the EMB are illustrated in Figs. 8, 9 and 10. The force excitations in the vertical direction are applied at Point A. As shown in these figures, the acceleration responses do not change much in the frequency range of 0.5-21.5 Hz, but decrease obviously in the frequency range of 21.5-250 Hz. However, the responses will increase slightly at about 275 Hz at the three bearings. In addition, the acceleration responses at the three bearings in the vertical direction are much larger than those in the horizontal direction, since the force excitations are applied in the vertical direction.

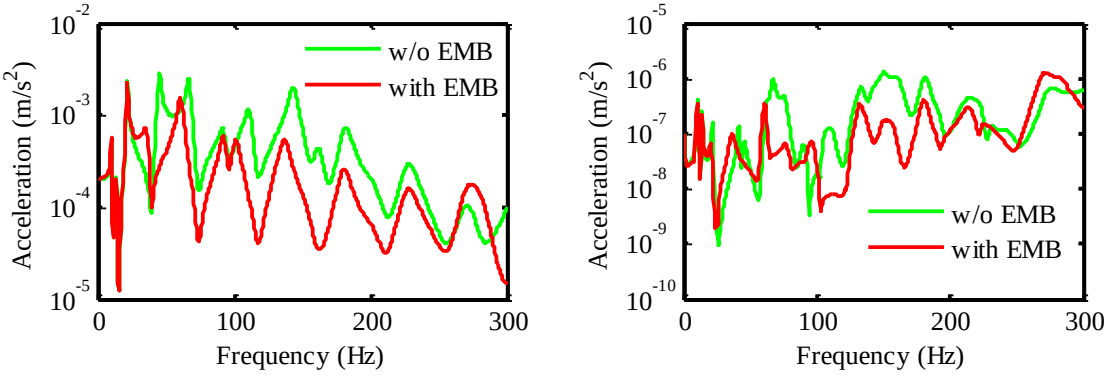

(a) Vertical. **(b) Horizontal.**

Figure 8: Vertical and horizontal acceleration responses of rear bearing to the unit vertical force.

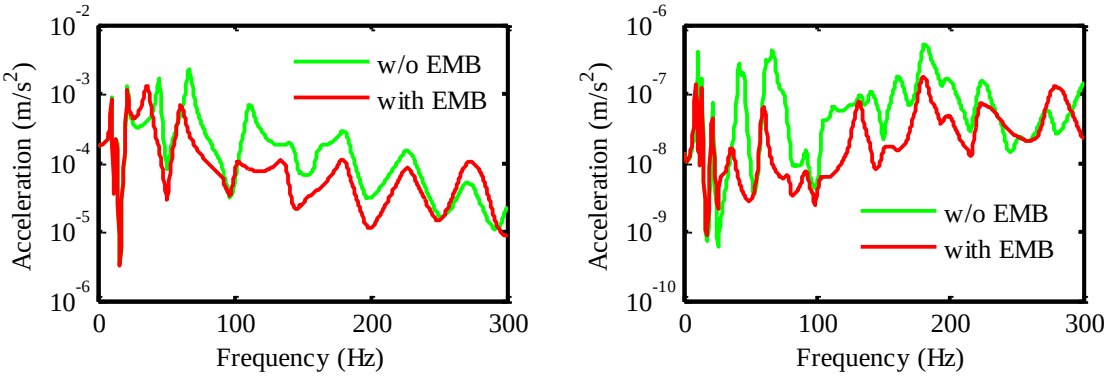

(a) Vertical. **(b) Horizontal.**

Figure 9: Vertical and horizontal acceleration responses of front bearing to the unit vertical force.

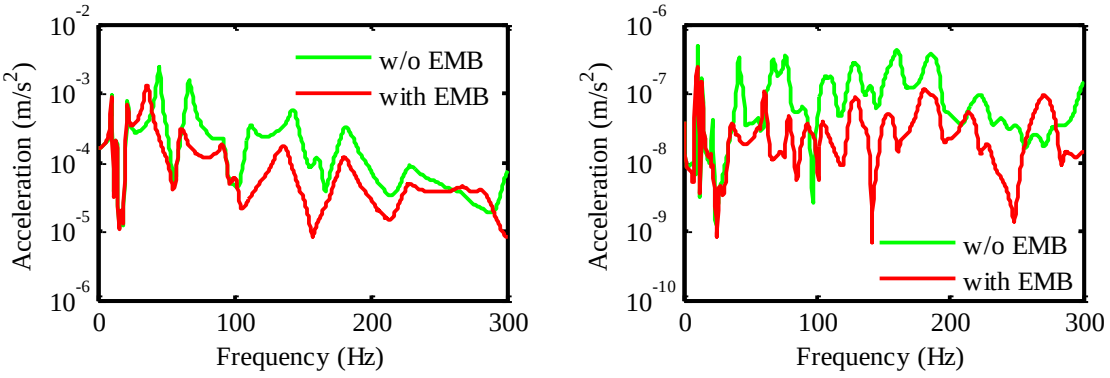

(a) Vertical. **(b) Horizontal.**

Figure 10: Vertical and horizontal acceleration responses of thrust bearing to the unit vertical force.

Acoustic radiation of the shaft-hull system in air to different force excitations is calculated by using the boundary element method (BEM), and the reference acoustic power is 10^{-12} W. As shown in Fig. 11, simulation results demonstrate that, when the EMB is placed in parallel with the rear bearing, the acoustic power is decreased substantially in the frequency range of 21.5-300 Hz in the

vertical and the horizontal directions, but it is magnified slightly at frequency 272 Hz (the vertical mode of the hull system) in the vertical direction and 226 Hz (the horizontal mode of the hull system) in the horizontal direction. In addition, it keeps roughly unchanged in the range of 0.5-21.5 Hz.

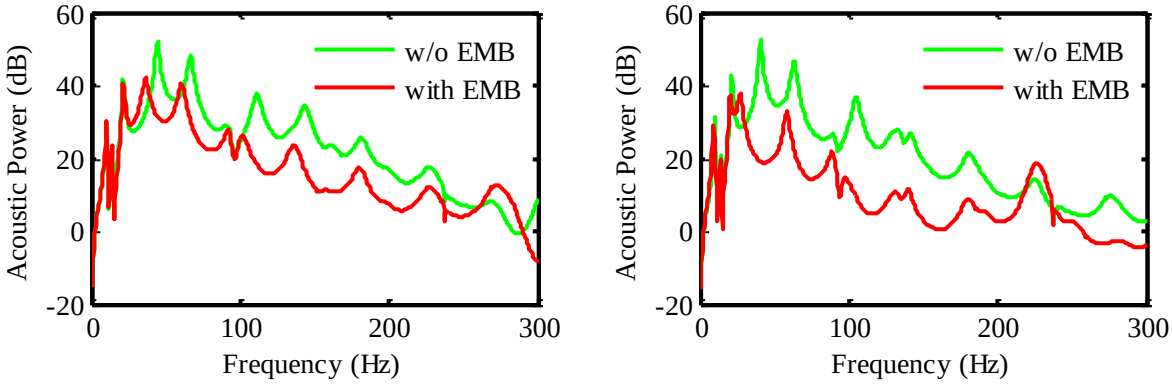

(a) Vertical. **(b) Horizontal.**

Figure 11: Acoustic power to the unit vertical and horizontal force.

In order to quantitate the reduction of the acoustic power when the EMB is placed in parallel with the rear bearing, the mean acoustic power levels are given in Table 2. The mean acoustic power levels are acquired by summing up the acoustic power to different frequencies in the whole frequency range of 0.5-300 Hz first and then calculating the acoustic power levels with the reference acoustic power 10^{-12} W. It is shown that the mean acoustic power levels achieve a reduction of about 6.7 dB to the unit force excitation in the vertical direction and 11.8 dB in the horizontal direction.

Table 2: Comparison of the mean acoustic power levels with or w/o EMB

Mean acoustic power level (dB)	Vertical force excitation	Horizontal force excitation
Without EMB	34.9	34.0
With EMB	28.2 (-6.7)	22.2 (-11.8)

5. Conclusions

Theoretical investigation on the vibration control of a shaft-hull system with electromagnetic bearings is presented. Dynamic characteristics of the electromagnetic bearing are analysed, and especially the equivalent stiffness and damping of the electromagnetic bearing are obtained. The frequency response synthesis method is employed to establish a mathematical model of the shaft-hull system and based on this model the influence of the EMB on the vibration transmission and acoustic radiation is discussed. Simulation results demonstrate that interfacial forces at the three bearings in the vertical and horizontal directions can be efficiently controlled when the electromagnetic bearing is introduced into the shaft-hull system and located in parallel with the rear bearing. In addition, the acceleration responses at the three bearings will be reduced in the whole, and consequently, the acoustic power of the system is reduced.

Acknowledgements

This work was supported financially by the National Natural Science Foundation of China (Grant No.11672180 and No.11172166).

REFERENCES

1 Xie, J., Shen, S., Wu, Y. Research Status on Noise Radiation from Vibrating Hull Induced by Propeller and Reduction Measures, *Shipbuilding of China*, **51** (4), 234-241, (2010).

2 Hu, F. *Research on Active Control of the Longitudinal Vibration of Propulsion Shafting Systems*, Doctor of Philosophy dissertation, Shanghai Jiao Tong University, (2014).

3 Li, D. *Analysis and Experiment on Vibration and Acoustic Radiation of the Shafting-hull Coupled System*, Master of Engineering dissertation, Shanghai Jiao Tong University, (2012).

4 Hu, S. *Study on Vibration and Underwater Acoustic Radiation of Propeller-shaft-hull Coupled System under Control of the Longitudinal Vibration of Shafting*, Master of Engineering dissertation, Shanghai Jiao Tong University, (2016).

5 Dylejko, P. G. *Optimum resonance changer for submerged vessel signature reduction*, Doctor of Philosophy dissertation, University of New South Wales, (2007).

6 Liu, G., Wu, W., Rao, C., and Chen, R. Numerical Calculation of Whirling Vibration of Ship Shafts Based on Transfer Matrices Method, *Chinese Journal of Ship Research*, **5**(1), 60-63, (2010).

7 Ji, C., Wang, J., Mo, G., Zou, J., and Yang, H. Instability of a poppet valve: interaction of axial vibration and lateral vibration, *The International Journal of Advanced Manufacturing Technology*, 1-10, (2016).

8 Javed, A., Mizuno, T., Takasaki, M., Ishino, Y., Hara, M., and Yamaguchi, D. Proposal of lateral vibration control based on force detection in magnetic suspension system, *International Journal of Applied Electromagnetics and Mechanics*, (Preprint), 1-7, (2015).

9 Kim, J., and Reddy, J. N. Analytical solutions for bending, vibration, and buckling of FGM plates using a couple stress-based third-order theory, *Composite Structures*, 103, 86-98, (2013).

10 Gerhard, S., and Eric, H. M. *Magnetic bearings: theory, design, and application to rotating machinery*, Springer, (2009).

11 Hu, Y., Zhou, Z., Jiang, Z. *Basic Theory and Application of Magnetic Bearing*, China Machine Press, Beijing, China, (2006).

12 Burdent, L. *Active magnetic bearing design and characterization for high temperature applications*, Doctor of Philosophy dissertation, EPFL, (2006).

13 Dong, L., and You, S. Adaptive control of an active magnetic bearing with external disturbance, *Isa Transactions*, **53** (5), 1410–1419, (2014).

14 Zhou, J., Di, L., Cheng, C., Xu, Y., and Lin, Z. A rotor unbalance response based approach to the identification of the closed-loop stiffness and damping coefficients of active magnetic bearings, *Mechanical Systems and Signal Processing*, 66, 665-678, (2016).

15 Mushi, S. E. *Robust control of rotor dynamic instability in rotating machinery supported by active magnetic bearings*, Doctor of Philosophy dissertation, University of Virginia, (2012).

16 Samsudin, S. I., Rahim, H. R. A., and Jahari, A. N. M. PD-Fuzzy Logic Controlled on a Magnetic Bearing System, *Journal of Mechanical Engineering and Technology*, **2** (1), 71-86, (2010).

17 Le, Y., Fang, J., and Wang, K. Design and optimization of a radial magnetic bearing for high speed motor with flexible rotor, *IEEE Transactions on Magnetics*, **51** (6), 1-13, (2015).

18 Filion, G., Ruel, J., and Dubois, M. R. Reduced-Friction Passive Magnetic Bearing: Innovative Design and Novel Characterization Technique, *Machines*, **1** (3), 98-115, (2013).

19 Yang, Z., Zhao, L., and Zhao, H. (2002). Global linearization and microsynthesis for high-speed grinding spindle with active magnetic bearings, *IEEE Transactions on Magnetics*, 2002, **38** (1):250-256.

20 Yang, G., Xu, Y., Shi, Z., and Gu, H. Characteristic analysis of rotor dynamics and experiments of active magnetic bearing for HTR-10GT, *Nuclear Engineering and Design*, **237** (12), 1363-1371, (2007).